ISSN (Print) 1226-1750
ISSN (Online) 2233-6656
Journal of Magnetics 20(4), 331-335 (2015) http://dx.doi.org/10.4283/JMAG.2015.20.4.331

First-principle Study for $Al_xGa_{1-x}P$ and Mn-doped $AlGaP_2$ Electronic Properties

Byung-Sub Kang and Kie-Moon Song*

Nanotechnology Research Center, Dept. of Nano Science and Mechanical Engineering, Konkuk University, Chungju 27478, Korea

(Received 31 July 2015, Received in final form 4 December 2015, Accepted 10 December 2015)

The ferromagnetic and electronic structure for the $Al_xGa_{1-x}P$ and Mn-doped $AlGaP_2$ was studied by using the self-consistent full-potential linear muffin-tin orbital method. The lattice parameters of un-doped $Al_xGa_{1-x}P$ (x = 0.25, 0.5, and 0.75) were optimized. The band-structure and the density of states of Mn-doped $AlGaP_2$ with or without the vacancy were investigated in detail. The P-3*p* states at the Fermi level dominate rather than the other states. Thus a strong interaction between the Mn-3*d* and P-3*p* states is formed. The ferromagnetic ordering of dopant Mn with high magnetic moment is induced due to the (Mn-3*d*)-(P-3*p*)-(Mn-3*d*) hybridization, which is attributed by the partially filled P-3*p* bands. The holes are mediated with keeping their 3*d*-characters, therefore the ferromagnetic state is stabilized by this double-exchange mechanism.

Keywords : chalcopyrite and luzonite, ferromagnetic half-metallicity, first-principle

1. Introduction

Diluted magnetic semiconductors (DMSs) have paid a great interest because the *s* and *p* electrons of the non-magnetic materials, and the spin from the magnetic dopant can be employed in spintronic devices. A recent strategy to achieve further control over the spin degree of freedom is based on dilute ferromagnetic (FM) semiconductors, prepared by substituting magnetic ions such as V, Cr, Mn, Fe, Co, and Ni into non-magnetic semiconductor hosts. Ferromagnetism has been reported in various semiconductor groups including II-VI [1, 2] and III-V [3-5] such as GaN, ZnO, and so on. The spin-polarization in the semiconductor has tended to disappear quickly by spin-flip scattering, when the charges of FM matters are implanted as spin injectors. It is a great worth to handle the FM semiconductors because the difficulty in the spin-injection to make DMSs at room temperature. The conventional DMS have had a low solubility of magnetic ions in host semiconductors. Accordingly, the opportunities of DMS application have been limited due to the low solubility of magnetic ions in non-magnetic semiconductor hosts.

An approach in enhancing the solubility is to make a monolayer super lattice [6], and another is to find a new pure FM semiconductor. Recently, newly synthesized a $MnGeP_2$ compound has been reported as a semiconductor, whose crystal structure is chalcopyrite. It has been reported that $MnGeP_2$ exhibits ferromagnetism with T_c = 320 K and a magnetic moment per Mn at 5 K of 2.58μ_B, and an indirect energy-gap of 0.24 eV. Moreover, it has been reported that the Mn-doped chalcopyrite such as $ZnSnAs_2$ [7] and $ZnGeP_2$ [8] shows FM ordering at 320 and 312 K, respectively. Chalcopyrite is a familiar tetrahedrally-coordinated zinc-blende material, which is a class of semiconductor confirmed as a promising material to fabricate nonlinear optical devices. In our works, we studied by using first-principle calculations for the electronic and magnetic properties of $(Al_{1-y}Mn_y)GaP_2$ and $Al(Ga_{1-y}Mn_y)P_2$ with y = 0.03125 and 0.0625 DMS without or with the defects. In Mn-doped chalcopyrite $AlGaP_2$ semiconductor, we observed FM ordering. The FM Mn-doped $AlGaP_2$ chalcopyrite is the most energetically favorable one. Total-energy calculations are predicted that the ternary compound $AlGaP_2$ is a semiconductor with direct band-gap of 1.237 eV. The spin polarized $Al(GaMn)P_2$ state (Al-rich) without the defects is more stable than that of $(AlMn)GaP_2$ state (Ga-rich) with the magnetic moment of about 3.8μ_B/Mn. The Mn-doped $AlGaP_2$ yields strong half-metallic ground states. We noted that this chalcopyrite and related materials can replace the Mn-doped $AlGaP_2$ system and open the way to room temperature spintronic devices.

*Corresponding author: Tel: +82-43-840-3620/3628
Fax: +82-43-851-4169, e-mail: kmsong@kku.ac.kr, kangbs@kku.ac.kr

2. Computational Details

The ab-initio calculations were performed using a self-consistent the full-potential linear muffin-tin orbital (FPLMTO) method based on the framework of the density-functional theory [9]. The radii of muffin-tin (MT) sphere radii for Mn/Ga (or Al) and P were chosen to be 2.4 (or 2.22) and 1.9 a.u., respectively. The final set of energies was computed with the plane-wave cutoff energy of 596.63 eV. The convergence tests of the total energy with respect to the plane-wave energy cutoff and k-point sampling had been carefully examined. Brillouin zone integrations were performed with the special k-point method over a gamma-centered $4 \times 4 \times 4$ mesh. It is corresponding to 64 k-points. It insured that the total energies and the magnetic moments were converged on a better 10 meV/cell and $0.01\mu_B$/atom scale, respectively. The exchange-correlation energy of the electrons was described in the generalized gradient approximation (GGA) as a function proposed in Perdew-Burke-Ernzerhof scheme [10].

The LMTO basis set and charge density in each MT sphere were expanded in real spherical harmonics up to $l = 6$, where l is the angular momentum defined inside each MT sphere. The LMTO basis functions for Mn and Ga atoms within the valence-energy region were chosen as 4*s* and 3*d*, and 4*s*, 4*p*, and 3*d*, respectively. The electron wave function was expanded in plane wave with a cut-off energy of 159.12 eV, 232.56 eV, and 340.0 eV for the Mn-4*s* (or Al-3*s*), Mn-4*p* (or Al-3*p*), and Mn-3*d*, respectively. The relativistic effect for the valence electrons was taken into account by the scalar-relativistic approximation. The MT approximation was employed in order to describe the atomic potential, the effects of spin-orbital coupling of valence electrons were not included. The atomic potentials were approximated by spherically symmetric potential. However, the full charge-density, including all non-spherical terms, was evaluated in Fourier series in the interstitial region on the FPLMTO method.

3. Results and Discussion

We considered the relaxations for the atomic sites of the structures. The equilibrium lattice parameters are a = 5.7255 Å and 5.6483 Å for $Al_xGa_{1-x}P$ ($x = 0$) and $Al_xGa_{1-x}P$ ($x = 1.0$), respectively. The total-energy minimization of the super-cell with keeping a $c/a = 2.0$ was performed. The calculated parameters for GaP and AlP can be compared with that of the zinc-blende structure. The experimental values are a = 5.451 Å and 5.450 Å for GaP [11, 12] and AlP [11], respectively. In the case of $Al_xGa_{1-x}P$, we considered the structural relaxation for each of a and c-axis. The equilibrium lattice parameters are a = 5.6845 Å, c = 11.2221 Å, and c/a = 1.974 at $x = 0.5$. The results of luzonite system with $x = 0.25$ and 0.75 are listed in Table 1. For the compositions $x = 0.25$ and 0.75 (luzonite), the simplest structure is an eight-atom simple cubic cell: the anions with the lower concentration form a regular simple cubic lattice. For the composition $x = 0.5$ (chalcopyrite), the smallest ordered structure is a four-atom tetragonal cell. Thus we considered the chalcopyrite structure, which has a 16-atom tetragonal cell. This structure is suitable for simulating random alloys. The considered system of Mn-doped $AlGaP_2$ with the Mn concentrations of 3.125% and 6.25% consists of 64 atoms (super-cell) included 32 empty sites (or interstitial sites) with one or two atoms substituted by Mn. The crystal structure of chalcopyrite $AlGaP_2$ in a unit-cell was displayed in the Fig. 1.

Table 1. Equilibrium lattice parameters (Å) and band-gap (E_g, eV) for $Al_xGa_{1-x}P$ ($x = 0.25$, 0.5, and 0.75).

$Al_xGa_{1-x}P$	Lattice Parameter (Å)		Ratio	Band-gap
x	a	c	c/a	E_g (eV)
0.25 Luzonite	5.7042	11.3228	1.985	0.7339
0.50 Chalcopyrite	5.6845	11.2221	1.974	1.2376
0.75 Luzonite	5.6664	11.1514	1.968	1.5316

These structures for $Al_{0.25}Ga_{0.75}P$, $Al_{0.5}Ga_{0.5}P$ ($AlGaP_2$),

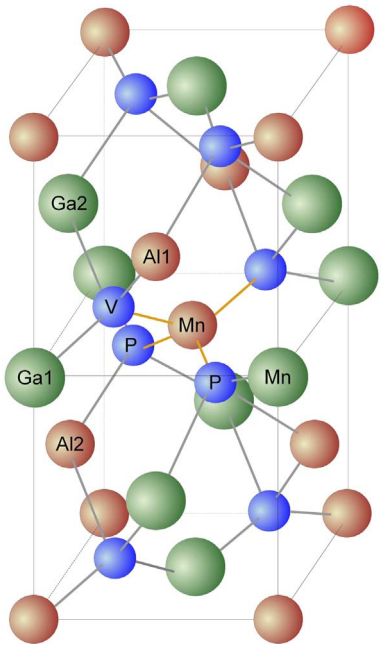

Fig. 1. (Color online) The unit-cell of chalcopyrite $AlGaP_2$. V represents the defect by P vacancy.

and $Al_{0.75}Ga_{0.25}P$ exhibit the semiconducting character with energy gaps of 0.7339 eV, 1.2376 eV, and 1.5316 eV, respectively. The band-gap increases as increases Al concentration in the $Al_xGa_{1-x}P$ system, while for the lattice parameter shows a downward bowing as increases Al concentration. In the case of pure $AlGaP_2$ with a vacancy of Al, Ga, or P atom, their energy-gaps disappear by the formation of defect states in the Fermi level (E_F). The calculated result of band-gap is smaller than that of the experiment [13]. It is general trend that the results by using the GGA are less than half of that in the experiment. Maybe it can be obtained the result that the calculated value in the local density approximation plus U procedure (Hubbard correction) [14] is slightly larger than that in the GGA.

The calculations for total energies in the $(Al,Mn)GaP_2$ system (Ga-rich) with replacing Al atoms by dopant Mn, in the $Al(Ga,Mn)P_2$ with replacing Ga atom by Mn (Al-rich), and in $AlGa(P,Mn)_2$ of P substitution by Mn were performed. The $Al(Ga,Mn)P_2$ is the lowest energetically favorable system. Its difference in their energies is small in comparison with these systems. In the case of without a vacancy, the substitution energies for the $(Al,Mn)GaP_2$, $Al(Ga,Mn)P_2$, and $AlGa(Mn_{0.5}P_{3.5})_2$ are –346.5 meV/Mn, –282.2 meV/Mn, and –270.7 meV/Mn, respectively. The defect energy ($E_{d,und}$) in un-doped system and the substitution energy ($E_{d,sub}$) with a vacancy of Al, Ga, or P were defined as, respectively.

$$E_{d,und} = [E(AlGaP_2;V(Al,Ga,P))] - [E(AlGaP_2) - n_1\mu_{Al} - n_2\mu_{Ga} - n_3\mu_P], \quad (1)$$

$$E_{d,sub} = [E(AlGaP_2;Mn, V(Al,Ga,P)) - n_4\mu_{Mn}] - [E(AlGaP_2) - n_1\mu_{Al} - n_2\mu_{Ga} - n_3\mu_P], \quad (2)$$

where, $E(AlGaP_2;V(Al,Ga,P))$ is the total energies of chalcopyrite $AlGaP_2$ with the vacancy of 3.125% concentration of host Al, Ga, or P atom. $E(AlGaP_2;Mn, V(Al,Ga,P))$ and $E(AlGaP_2)$ are the total energies of Mn-doped $AlGaP_2$ with a vacancy (of 3.125% concentration of Al, Ga, or P) and the perfect $AlGaP_2$ for the super-cell of the same size, respectively. The μ_{Mn}, μ_{Al}, μ_{Ga}, and μ_P are the atomic chemical-potentials of Mn, Al, Ga, and P. The integer n_1, n_2, n_3, and n_4 are the number of substituted Al, Ga, and P atoms, and doped Mn atoms. The atomic chemical-potentials depend on the experimental conditions. The relationship $\mu_{Al} + \mu_{Ga} + 2\mu_P = \mu_{AlGaP2}$ is formulated in thermal equilibrium with $AlGaP_2$. The μ_{Mn} will be determined by the equilibrium of bulk MnP in the FM phase. $\mu_{Al} = E(AlP) - E(P)$ and $\mu_{Ga} = E(GaP) - E(P)$ in the bulk system. For Al-rich system, $\mu_{Mn} = E(MnP) - E(AlP) + E(Al)$ and $\mu_P = E(AlP) - E(Al)$ in the bulk system; and for Ga-rich system, $\mu_{Mn} = E(MnP) - E(GaP) + E(Ga)$ and $\mu_P = E(GaP) - E(Ga)$ in the bulk system.

Table 2. Defect energies ($E_{d,und}$, eV) for un-doped $AlGaP_2$ and substitution energies ($E_{d,sub}$, eV) for Mn-doped $AlGaP_2$ with the vacancy of 3.125% Al, Ga, or P concentration. The delta (D) denotes the total energy difference between the substitution and defect energies. The parentheses are the Mn magnetic moment per one atom within the FM state.

Vacancy	$E_{d,und}$ (eV)	$E_{d,sub}$ (eV)	Δ (meV)
Al	8.4326	8.7061 (3.5μ_B)	+273.5
Ga	7.7360	7.8954 (3.4μ_B)	+159.4
P	9.2949	8.9896 (4.2μ_B)	–305.3

The FM state for Al-rich $Al(Ga_{3.0}Mn_{1.0})P_2$ system is more energetically favorable than the non-magnetic or antiferromagnetic (AFM) state. The Mn dopant orders ferromagnetically in $AlGaP_2$. The difference in total energy between the FM and AFM states is –34.72 meV in the Mn concentration of 6.25%. For $Al(Ga_{3.0}Mn_{1.0})P_2$, the nearest neighboring four surrounding P atoms formed the MnP_4 tetrahedron are aligned positively with magnetic moments of 0.05μ_B per P atom. While for the nearest neighboring Al or Ga atoms, it is aligned negatively with magnetic moment of about –0.02μ_B per Al or Ga atom. The substituted Mn atom has a high magnetic moment of about 3.8μ_B/Mn. In the case of P vacancy in $AlGaP_2$, the total-energy difference between the substitution energy by Mn and defect energy, $E_{d,sub} - E_{d,und}$, is the lowest by –0.305 eV. The Mn magnetic moment for Mn-doped $AlGaP_2$ with a vacancy is increased by 4.2μ_B/Mn more than that without a vacancy. These results were listed in the Table 2.

Figure 2 shows the band structures for 3.125% Mn-doped $AlGaP_2$ without defect, with Al, Ga, or P vacancy site in the FM state. The substituted system of Ga by Mn atom shows the half-metallic character due to downward shift of the host Al, Ga, and P minority bands (without defect system). The electronic properties near the E_F provide the information of the magnetic properties and their characteristics. It can be observed the perturbation of the valence-band by dopant Mn in Mn-doped $AlGaP_2$. The host (Al, Ga, and P atoms) band dispersions are significantly changed by the presence of the Mn dopant. A Mn-induced spin-splitting of the valence-band maximum is weak, but it can be observed from the density of states (DOS) or the band pictures. The perturbations of host atoms are stronger in the case of Ga-rich system than in that of Al-rich one. The Mn band shows a large exchange splitting because it is larger than the crystal-field splitting. The band of majority state on

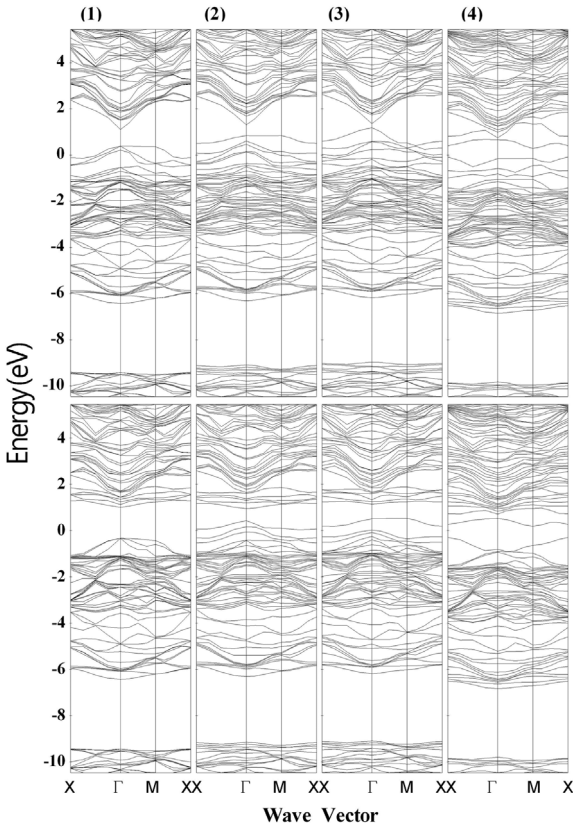

Fig. 2. Band structures for 3.125% Mn-doped $AlGaP_2$ (1) without defect, (2) with Al defect, (3) with Ga defect, and (4) with P defect site in the FM state. The concentration of defect is 3.125%. Up-four-panel represents the majority-spin state. Down-four-panel represents the minority-spin state. The Fermi level is set to zero.

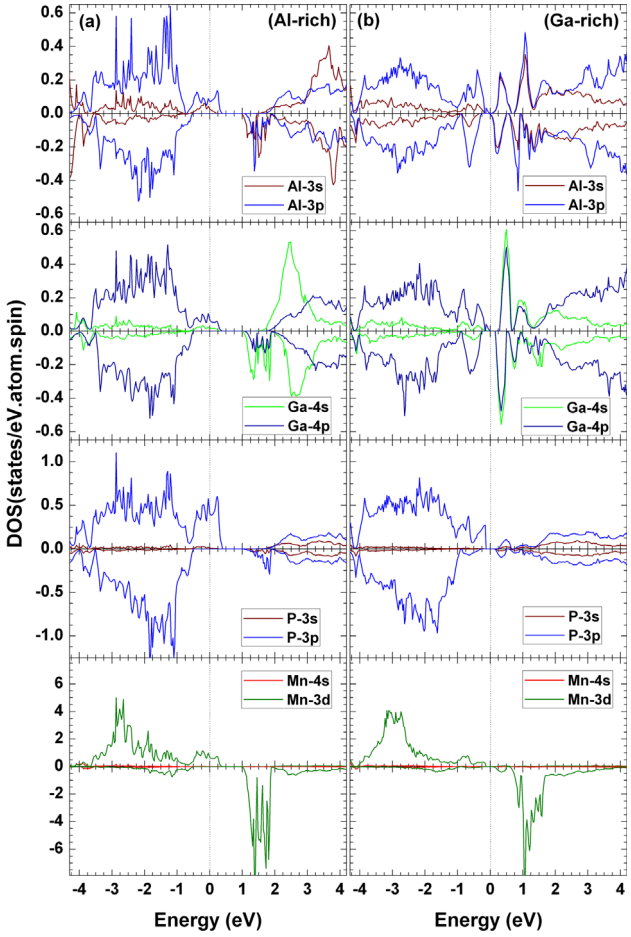

Fig. 3. (Color online) (a) DOS for Al, Ga, P, and Mn sites of Al-rich $Al(GaMn)P_2$ (6.25% Mn) in the FM state. (b) DOS for Al, Ga, P, and Mn sites of Ga-rich $(AlMn)GaP_2$ (3.125% Mn) with a vacancy of P in the FM state. The Fermi level is set to zero.

the E_F occupies Al-3*p* and Ga-4*p*, and P-3*p* electrons mainly. These majority *p* states make a result of strong hybridization between the P-3*p* (or Al-3*p*, or Ga-4*p*) and Mn-3*d* bands. Fig. 3 shows the density of states (DOS) for Al-rich $Al(GaMn)P_2$ of 6.25% Mn and for Ga-rich $(AlMn)GaP_2$ with a P vacancy of 3.125% concentration. For Al-rich $Al(GaMn)P_2$ of 6.25% Mn, we can observe the FM half-metallicity. This half-metallicity is due to the Mn-3*d* states hybridize well with the P-3*p* state. The holes are itinerant with keeping their d-character due to the hybridization with the Mn-3*d* states. Therefore the kinetic energy is lowered so efficiently that the FM state is stabilized by the double-exchange mechanism. Hence the partially filled P-3*p* band and a defect P bands contribute to the ferromagnetism with high magnetic moment. These configurations provide us with clues to elucidate the mechanism of the hole-mediated ferromagnetism. The Mn-P bond in $Al(GaMn)P_2$ is largely covalent because a strong interaction between the Mn-3*d* and P-3*p* states. When it exhibits the substitution of Al or Ga by Mn, the Mn and P atoms forms the Mn-P-Mn bond. The strong hybridization between P-3*p* and Mn-3*d* states is reduced in the vacancy-system of P. A high magnetic moment of Mn is maintained.

4. Conclusions

We had investigated the electronic structure and magnetic properties of the $Al_xGa_{1-x}P$ ($x = 0.25$, 0.5, and 0.75) and Mn-doped chalcopyrite $AlGaP_2$ semiconductor by using the first-principles calculations. The chalcopyrite $AlGaP_2$ compound is a *p*-type semiconductor with a band-gap of 1.2376 eV. For Mn-doped $AlGaP_2$, we had observed that this system exhibits the FM and half-metallic ground state with respect to the Mn-doping concentration. The ferromagnetism of dopant Mn is induced by the partially filled P-3*p* bands. The high magnetic moment of Mn is maintained by the hybridized (Mn-3d)-(P-3*p*)-(Mn-3*d*)

interaction. Accordingly, the FM state is stabilized by the double-exchange mechanism from the hybridization between the Mn-3*d* state and the hole-mediated P-3*p* states.

Acknowledgements

This work was supported by Konkuk University (Dept. of Nano science and Mechanical engineering) in 2015.

Rerefences

[1] T. Fukumura, Zhengwu Jin, A. Ohtomo, H. Koinuma, and M. Kawasaki, Appl. Phys. Lett. **75**, 3366 (1999).
[2] K. Sato and H. Katayama-Yoshida, Phys. Stat. Sol. (b) **229**, 673 (2002).
[3] Priya Mahadevan and Alex Zunger, Phys. Rev. B**69**, 115211 (2004).
[4] X. Y. Cui, J. E. Medvedeva, B. Delley, A. J. Freeman, and C. Stampfl, Phys. Rev. B**75**, 155205 (2007).
[5] S. J. Pearton, C. R. Abernathy, D. P. Norton, A. F. Hebard, Y. D. Park, L. A. Boatner, and J. D. Budai, Mater. Sci. and Engin. R **40**, 137 (2003).
[6] J. Choi, S. Choi, S. C. Hong, S. Cho, M. H. Sohn, Y. Park, K. W. Lee, H. Y. Park, J. H. Song, and J. B. Ketterson, J. of Korean Phys. Soc. **47**, S497 (2005).
[7] S. Choi, G.-B. Cha, S. C. Hong, S. Cho, Y. Kim, J. B. Ketterson, S.-Y. Jeong, and G.-C. Yi, Solid State Comm. **122**, 165 (2002).
[8] Sunglae Cho, Sungyoul Choi, Gi-beom Cha, Soon Cheol Hong, Yunki Kim, Yu-Jun Zhao, Arthur J. Freeman, John B. Ketterson, B. J. Kim, Y. C. Kim, and Byung-Chun Choi, Phy. Rev. Lett. **88**, 257203-1 (2002).
[9] S. Y. Savrasov, Phys. Rev. B**54**, 16470 (1996), and references therein.
[10] J. P. Perdew, K. Burke, and M. Ernzerhof, Phys. Rev. Lett. **77**, 3865 (1996).
[11] C. Kittel, Introduction to Solid State Physics Seventh ed., John Wiley & Sons (1996).
[12] Nadir Bouarissa, Materials Chemistry and Physics, **124**, 336 (2010).
[13] S. J. Pearton, C. R. Abernathy, D. P. Norton, A. F. Hebard, Y. D. Park, L. A. Boatner, and J. D. Budai, Mater. Sci. and Eng. R **40**, 137 (2003).
[14] J. H. Park, S. K. Kwon, and B. I. Min, Physica B **281**&**282**, 703 (2000).